Journal of Applied Physics ARTICLE scitation.org/journal/jap

Advanced photo-assisted capacitance–voltage characterization of insulator/wide-bandgap semiconductor interface using super-bandgap illumination

Cite as: J. Appl. Phys. **125**, 175704 (2019); doi: 10.1063/1.5089793
Submitted: 23 January 2019 · Accepted: 13 April 2019 ·
Published Online: 2 May 2019

Atsushi Hiraiwa (平岩 篤),[1,2,a)] Satoshi Okubo (大久保 智),[3] Kiyotaka Horikawa (堀川 清貴),[3] and Hiroshi Kawarada (川原田 洋)[2,3,4]

AFFILIATIONS

[1]Institute of Materials and Systems for Sustainability (Tokyo Branch), Nagoya University, Bldg. 120-5 (Waseda University), 513 Waseda-tsurumaki, Shinjuku, Tokyo 162-0041, Japan
[2]Research Organization for Nano and Life Innovation, Waseda University, 513 Waseda-tsurumaki, Shinjuku, Tokyo 162-0041, Japan
[3]Faculty of Science and Engineering, Waseda University, 3-4-1 Okubo, Shinjuku, Tokyo 169-8555, Japan
[4]The Kagami Memorial Laboratory for Materials Science and Technology, Waseda University, 2-8-26 Nishiwaseda, Shinjuku, Tokyo 169-0051, Japan

[a)]**Electronic addresses:** hiraiwa@aoni.waseda.jp and qs4a-hriw@asahi-net.or.jp

ABSTRACT

To accurately analyze the deep states at the insulator/wide-bandgap semiconductor interface, this study reassessed and improved the conventional photoassisted capacitance–voltage (PACV) method. First, as previously pointed out, the illumination time under depletion should be long enough that the voltage shift caused by interface-state depopulation (in *n*-type semiconductors) saturates. Excessive illumination, however, causes insulator charging, thereby apparently increasing estimated values. To solve this problem, this study proposes to measure reference characteristics just after postillumination ones. Secondly, the postillumination measurements should be started without delay after turning off the light or may be carried out with the samples being illuminated. Thirdly, the depletion should be deep enough that the magnitude of band bending in the substrate at the beginning of the postillumination measurements is larger than 1 V. This guideline considerably relaxes a previous one that required a band bending of bandgap or larger. Furthermore, this study developed a method for compensating the interface-state depopulation (in *n*-type) during the reference measurements, in which the depopulation causes the so-called stretch-out. The results thus obtained from an $Al/Al_2O_3/GaN$ capacitor agreed fairly well with those by a recently developed transient photoassisted capacitance method, supporting the validity of both methods. Being less sensitive to the gate-insulator charging, the advanced PACV method developed here has an advantage over the transient method and, therefore, will help advance the technology for fabricating high-performance, high-reliability insulator/wide-bandgap semiconductor insulators.

I. INTRODUCTION

Compared to the industry-standard material of Si,[1] wide-bandgap semiconductors (WBGSs) have many superior properties such as high breakdown voltage, small intrinsic carrier density even at high temperatures, and high carrier mobility. Therefore, they have been extensively investigated to be applied to power control, high-frequency signal processing, and display devices. As a gate stack similar to the well-established thermal SiO_2/Si system[2] is not available, high-performance, high-reliability surface passivation, and gate insulation are major challenges here. The insulators for this purpose need to have good interface properties with the semiconductors, i.e., low level of interface states. Hitherto, the interface states have been mostly characterized by using capacitance–voltage (C–V) methods, such as the quasistatic method,[3] the Terman

method,[4] the high-low frequency method,[5] and the conductance method.[6] These methods are based on the prerequisite that, e.g., in *n*-type semiconductors, the interface-state-trapped electrons are in thermal equilibrium with conduction-band electrons, with holes being neglected owing to the wide bandgap. Because of this requirement, the range of interface-state detection is limited, at the deepest, to approximately 1 eV below the conduction band edge,[7] leaving a majority of insulator/WBGS interface states undetected. To solve this problem, a photoassisted *C*–*V* (PACV) method was proposed in several studies,[7–10] where, in *n*-type semiconductors, the deep as well as shallow interface states are depopulated by the photoexcitation of the trapped electrons and by the recombination of the electrons with photogenerated inversion holes. Then, the total number of interface states across the bandgap is estimated from the *C*–*V*-characteristic shift caused by the depopulation. Despite its success in detecting the interface states, there remain serious concerns about the validity of the obtained results, as explained below. First, the *C*–*V*-characteristic shift in most studies varied with the capacitance at which it was read, spoiling the consistency and the objectivity of the analysis. Some reports[11,12] used this capacitance-dependent shift to estimate the interface-state distribution in the bandgap in a manner similar to the Terman method. This method, however, only yields accurate results near the conduction-band edge, as well as the Terman method. Given that both this and the Terman method are based on the aforementioned thermal-equilibrium prerequisite, this similarity of detection limit for both methods is quite reasonable. Secondly, the measurement conditions, such as the gate voltage to deplete the substrate during the illumination, do not seem to have been optimized. Finally, although known as causing *C*–*V* stretch-out,[2] the interface-state depopulation (in *n*-type semiconductors) during the measurement of reference *C*–*V* characteristics, from which the *C*–*V*-characteristic shifts are estimated, has not even been paid attention to in PACV analysis. This study aims at improving the PACV analysis as follows. First, the effect of the PACV measurement conditions, i.e., illumination time, hold time after illumination to start the postillumination *C*–*V* measurements, and depletion gate voltage, on the analyzed results is investigated. The precedent works[10,12] already did this, but mostly focused on shallow defects, as mentioned above. Therefore, this study re-examines the PACV conditions from a viewpoint of their impact on deep-interface-state analysis. Then, based on the results, a more adequate guideline for accurate PACV analysis is presented. Finally, the long-overlooked problem of the stretch-out effect of reference *C*–*V* characteristics is assessed, and a method for its correction is proposed.

II. EXPERIMENTAL METHODS

A. Sample preparation

This study investigated metal-insulator-semiconductor (MIS) capacitors that were formed in the same manner as those of our previous study,[13] as summarized in what follows. The substrates were 0.3-mm-thick, *c*-plane, *n*-type low-resistivity (<30 mΩ cm) GaN plates with 2-μm-thick *n*-type homo-epitaxial layers doped with 5.5×10^{16} cm^{-3} Si. After successive cleaning in organic solvents, a piranha solution, and a 6% HCl solution, 33-nm-thick Al_2O_3 films were deposited on the substrates by atomic layer deposition (ALD) at 450 °C using trimethylaluminum and H_2O as precursors. The Al_2O_3 films formed under this condition have excellent passivation capability[14] and high breakdown reliability.[13] On the Al_2O_3 films, Al gate electrodes were formed by resistance-heating-type vacuum evaporation using a shadow mask with openings of a diameter of 339 μm. The effective gate area was 9×10^{-4} cm^2. Finally, after etching the backsides of substrates by using ion beam, Ohmic contacts were formed to the backsides by successive ion-beam depositions of Ti and Au using another shadow mask. Neither postdeposition nor postmetallization annealing was applied in this study.

B. Measurements

The capacitance of the Al_2O_3 MIS capacitors was measured under the amplitude and frequency of signal modulation of 30 mV and 1 MHz, respectively, using a B1520A multifrequency capacitance measurement unit embedded in a B1500A Semiconductor Device Analyzer (Keysight Technology). This modulation frequency is high enough to keep the undesirable contribution from interface states below the level in conventional Terman method analyses, without sacrificing measurement accuracy owing to the aforementioned low-resistivity substrates. The equivalent SiO_2 thickness (EOT) of the Al_2O_3 films was estimated by fitting the theoretical *C*–*V* characteristics of MIS capacitors to the measured ones under deep accumulation ($V_G = +13$ V) to avoid the stretch-out effect caused by shallow interface states. For simplicity, the two-dimensional quantum mechanical effect[15] was not considered here, thereby overestimating EOT by less than 0.2 nm.[16,17] Although it did not have a significant role in this study, the thickness of the Al_2O_3 films was estimated to be 33 nm by spectroscopic ellipsometry, measuring Al_2O_3 films that were deposited on Si substrates simultaneously with those on GaN substrates. The EOT estimated by using this thickness and the dielectric constant 8.8 of the Al_2O_3 films[18] was 14.6 nm, which is approximately equal to the aforementioned *C*–*V* fitting value. This consistency supports the aforementioned deep-accumulation fitting for EOT estimation. The fitting value was adopted in this study, as explained later (Sec. III A).

C. Photoassisted capacitance–voltage measurements

A deuterium–halogen light source and a 350-nm longpass filter were used to irradiate the samples with the light of under 3.5 eV, which generated electron–hole pairs in the GaN substrates with a bandgap of 3.4 eV.[19] As schematically shown in Fig. 1, two types of time sequence of lighting and voltage control of MIS capacitors, lighting A and B, were adopted here. In lighting A, at time (a) in Fig. 1, the MIS capacitors were first pulled down to an accumulation state to fill all interface states with electrons, as schematically shown in Fig. 2(a). For simplicity, the charge neutrality level in Fig. 2 is assumed to be at the valence band edge, but it should be noted that the results in what follows were obtained without this assumption. The time t_{acc} spent on this accumulation was approximately 8 s. Then, the capacitors were pulled up to a depletion state, where conduction-band electrons were swept away, and a hole inversion layer started to be generated owing to the super-bandgap light. At time (b) in Fig. 1, the capacitors were kept under the same gate voltage, with interface-state-trapped electrons gradually being photoemitted and recombining with the inversion

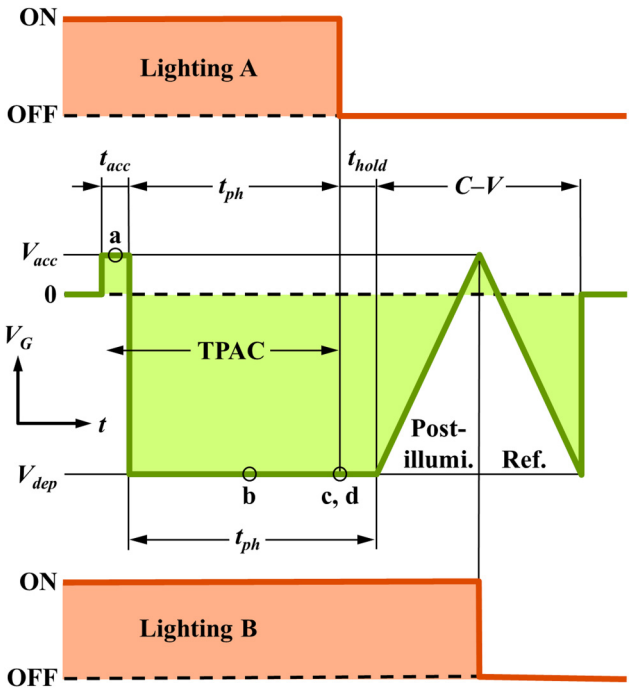

FIG. 1. Timing chart of PACV measurements. A deuterium–halogen light source and a 350-nm longpass filter were used to irradiate the samples with the light of under 3.5 eV, which is large enough to generate electron–hole pairs in the GaN substrates. Contrary to previous studies, the reference *C–V* characteristics in this study were measured after postillumination ones. The period from time a to c is available for TPAC measurements without disturbing the PACV measurements. The band diagrams of a MIS capacitor at times a–d are shown in panels (a)–(d) in Fig. 2, respectively.

holes in parallel [Fig. 2(b)]. At time (c) in Fig. 1, after all the interface states were depopulated, the light source was turned off [Fig. 2(c)], and, without much delay, *C–V* measurements were started from the aforementioned depletion state to the accumulation state, being followed by the reverse scanning. The time for this delay is called *hold time* in what follows. By contrast, in lighting B, the light source was kept lit during the first half of the *C–V* measurements. Unlike the conventional PACV measurements, the reference (accumulation to depletion) *C–V* characteristics were measured without delay after the postillumination (depletion to accumulation) ones. The merit of this measurement sequence is examined in Sec. III A.

III. RESULTS

A. Choice of illumination time

Figure 3 shows the PACV characteristics of an Al_2O_3 MIS capacitor for various illumination times under a depletion gate voltage of −12 V. The accumulation voltage was +2 V here and in what follows. The lighting was in mode B, and the illumination time ranged from 5 to 900 s. The postillumination capacitance, as represented by the dotted and the dashed lines, increased and eventually saturated with illumination time, indicating that the interface states were certainly depopulated by light. By contrast, the values of reference capacitance for illumination time of 5 and 900 s, as represented by the thick and the thin solid lines (black in color printing), respectively, were not much different between the two, serving as a reference. The results similar to those in Fig. 3 were previously reported, but only revealed a narrow aspect of the effect of illumination time.[11] Therefore, this effect is more comprehensively investigated here. The gate voltage shift ΔV_G yields the quasitotal interface-state density $N_{it,QBG}$ across the bandgap, as

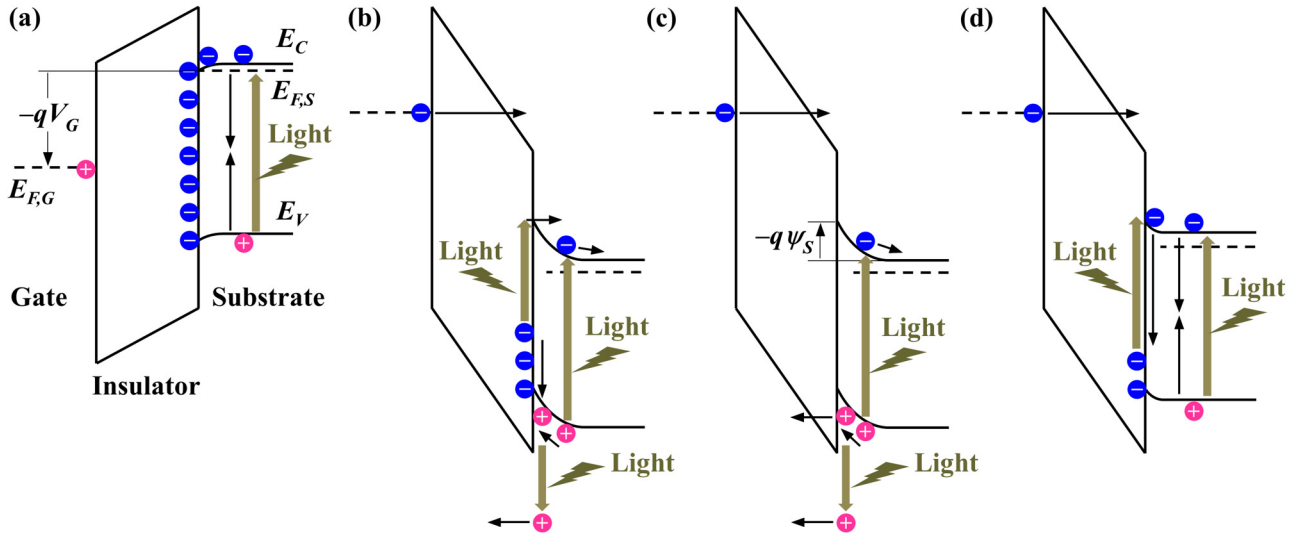

FIG. 2. Band diagrams of a MIS capacitor under PACV measurements. Panels (a)–(d) show the states of the capacitor at times a–d in Fig. 1, respectively. For simplicity, the charge neutral level is assumed to be located at the valence band edge. Panel (d) also shows the state at time c but under a smaller magnitude of depletion gate voltage than panel (c).

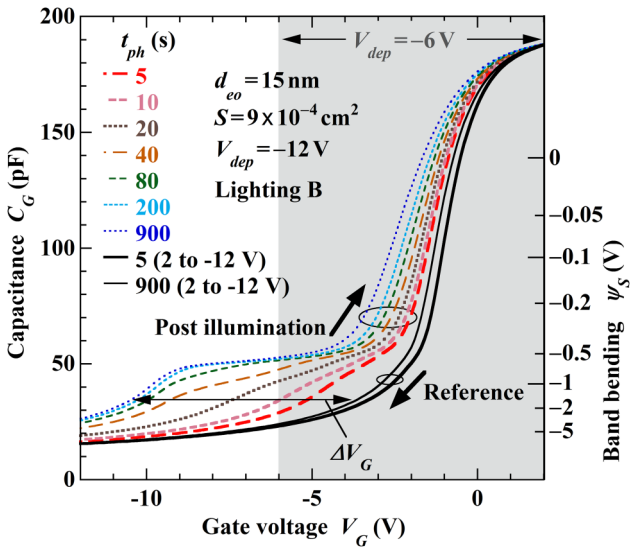

FIG. 3. PACV characteristics of an Al/Al_2O_3/GaN capacitor for various illumination times. The EOT and the area of the capacitor were 15 nm and 9 × 10^{-4} cm^2, respectively, here and in what follows. The sample was illuminated in mode B under the depletion gate voltage of −12 V. The postillumination results for illumination time of 5–900 s are shown here, as represented by the dashed and dotted lines. The thick and the thin solid lines (black in color printing) represent the reference characteristics measured after the postillumination ones for illumination time of 5 and 900 s, respectively. For reference, the portions in the shadowed area approximately show the results that are expected for a depletion gate voltage of −6 V. The results for other depletion gate voltages are similarly estimated. The band bending in the substrate, calculated by using Eq. (2), is shown by the right vertical axis.

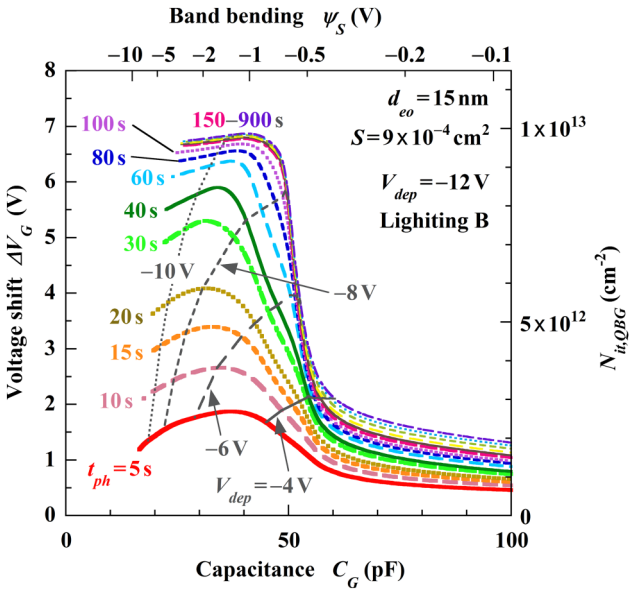

FIG. 4. Voltage shifts for various illumination times as a function of capacitance at which the shifts are read. Some of the results here were obtained by using the data given in Fig. 3. The quasitotal interface-state density, obtained by using Eq. (1), is shown by the right vertical axis. The thin lines (gray in color printing) represent the left boundaries of the results that are expected for a depletion gate voltage of –4 to –10 V.

given by[7,8]

$$N_{it,QBG} = c_{ins}\Delta V_G/q, \tag{1}$$

where c_{ins} is the gate-insulator capacitance per unit area, defined by $c_{ins} = \varepsilon_{ins}/d_{ins}$ with ε_{ins} and d_{ins} being the permittivity and the thickness of the gate insulator, respectively, and q is the electronic charge. To be exact, the contribution from some layer, such as GaO_x possibly intervening between the Al_2O_3 film and the GaN substrate, should be contained in the gate-insulator capacitance, i.e., $c_{ins} = 1/(d_{AlO}/\varepsilon_{AlO} + d_{GaO}/\varepsilon_{GaO})$, where d_{AlO} and ε_{AlO} are the thickness and permittivity of Al_2O_3, respectively, and d_{GaO} and ε_{GaO} are those of GaO_x. As this task is not easy, c_{ins} is more conveniently and more accurately estimated by $c_{ins} = \varepsilon_{SiO}/d_{eo}$, where ε_{SiO} is the permittivity of thermal SiO_2 (=3.9 ε_0 with ε_0 being the vacuum permittivity) and $d_{eo} = \varepsilon_{SiO}$ $(d_{AlO}/\varepsilon_{AlO} + d_{GaO}/\varepsilon_{GaO})$ is the gate insulator EOT, being estimated to be 15 nm in this study as mentioned earlier (Sec. II B). The reason why the value given by Eq. (1) is called quasitotal is explained later (Sec. III D). According to a separate report,[20] the contribution of inversion holes was neglected in Eq. (1). The validity of this neglect is also examined later in Sec. IV. Figure 4 shows the voltage shifts, some of which were obtained by using the results shown in Fig. 3, as a function of capacitance at which the voltage shifts are read. For reference, the quasitotal interface-state densities, estimated by using Eq. (1), are shown by the right vertical axis of the figure. The voltage shift in the small-capacitance range for illumination time of 100 s and longer is approximately independent not only of the illumination time but also of the capacitance, facilitating accurate analysis. The saturation of the voltage shift is more clearly seen in Fig. 5, where the circles represent the shifts for the minimum capacitance in Fig. 4 as a function of illumination time. The merit of investigating this type of voltage shift is also explained later (Sec. III D). For reference, the minimum capacitance in the postillumination characteristics is the one measured first. In Fig. 5, the result by a transient photoassisted capacitance (TPAC) method[20] is also shown, as represented by the triangles. This TPAC result was measured during the illumination period in the aforementioned PACV measurements, showing the deviation of interface-state-charge number density of the Al_2O_3 MIS capacitor from its initial value. In principle, this deviation is also equal to the quasitotal interface-state density across the bandgap in the limit of a long illumination time. Actually, however, the deviation shown in Fig. 5 kept linearly increasing for extended illumination, possibly being caused by hole trapping at Al_2O_3 traps with a relatively long lifetime, such as border traps. By contrast, in PACV analysis, the amounts of Al_2O_3 charging in the postillumination and the reference characteristic were approximately equal to each other, and, therefore, the Al_2O_3 charging effect was canceled out owing to the subtraction for obtaining the shift. However, even the PACV result slightly increased linearly with illumination time, supposedly due

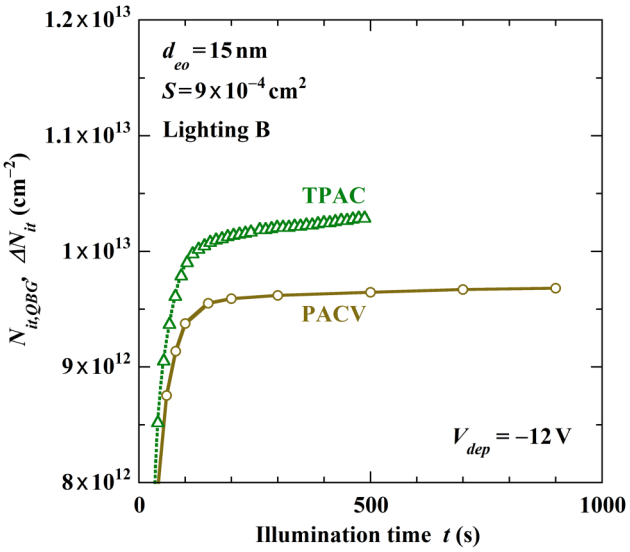

FIG. 5. Quasitotal interface-state density as a function of illumination time. The circles represent the results obtained for the smallest capacitance in Fig. 4. For reference, the triangles represent TPAC-analyzed interface-state-charge number densities as a function of illumination time.[20] The linear increase in the TPAC results observed after 150 s was ascribed to Al_2O_3 charging, whereas the PACV result only exhibited a slight increase owing to the reference *C*–*V* characteristics measured after the postillumination ones, as shown in Fig. 1. The lines simply connect the data points.

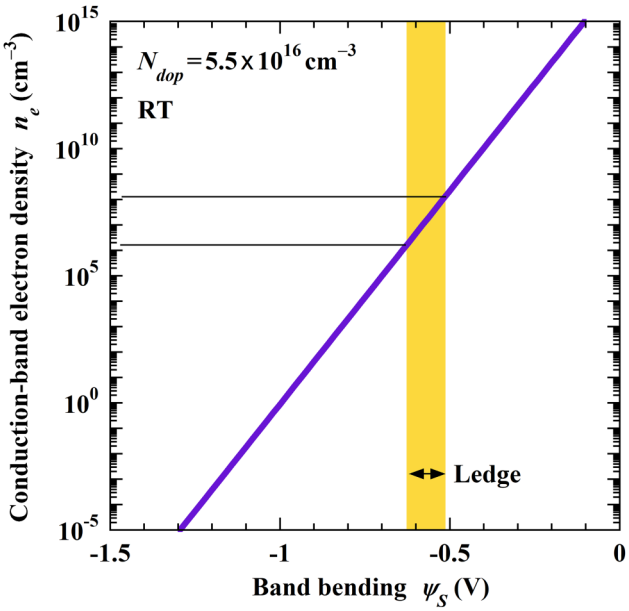

FIG. 6. Conduction-band electron density in the substrate near the insulator/substrate interface as a function of band bending. The electron density was calculated assuming the substrate doping concentration to be 5.5 × 10^{16} cm^{-3}. The band bending of −0.51 to −0.63 V for the ledges observed in Fig. 9 is colored.

to the discharging of the holes at Al_2O_3 traps during the postillumination and the reference measurement, especially for the gate voltages near accumulation condition, where there exist many conduction-band electrons available for the recombination with holes. For reference, the Al_2O_3 charge in the PACV measurements is supposed to be approximately equal to that just after the prior TPAC measurement and to be discharged during the initial accumulation period for 8 s (time a in Fig. 1) in the next TPAC/PACV measurement.

To investigate the cause of the decrease in the voltage shift for capacitance of over 50 pF in Fig. 4, the band bending (surface potential) ψ_S in the substrate was estimated as a function of gate capacitance C_G by using the equation[11,20]

$$\psi_S = -\frac{\varepsilon_S q N_{dop}}{2}\left(\frac{S}{C_G} - \frac{1}{c_{ins}}\right)^2, \tag{2}$$

where ε_S and N_{dop} are the permittivity [=8.9 ε_0 (Ref. 21)] and the doping concentration (=5.5 × 10^{16} cm^{-3}) of the substrate, respectively, and S is the gate area (=9 × 10^{-4} cm^2). The estimated results are shown by the right vertical axis and by the upper horizontal axis in Figs. 3 and 4, respectively. As clearly shown in Fig. 4, the voltage shift markedly decreased for band bending of over −0.6 V ($|\psi_S| < 0.6$ V). As shown in Fig. 6,[20] for this band bending, electrons with a concentration of over 10^6 cm^{-3} exist in the conduction band of the substrate near the insulator/substrate interface. They recombine with inversion holes and are captured by empty interface states, as schematically shown in Fig. 2(d), thereby reducing the voltage shift. For reference, the electron density n_e in Fig. 6 was calculated by using $n_e = N_{dop}\exp[q\psi_S/(kT)]$, where k and T are the Boltzmann constant and temperature, respectively. In any case, given that the once depopulated interface states are remarkably repopulated under the band bending of −0.6 V and larger, the voltage shift should be read at the capacitance for which the band bending is smaller than −1 V, i.e., $|\psi_S| > 1$ V. The range of band bending of larger than −1 V, where accurate analysis is not expected, is named "error zone" in this study.

B. Choice of hold time

The second key condition of PACV measurement is the hold time, which is spent after turning off the light source until the reference *C*–*V* measurements are started. To investigate its effect, Fig. 7 shows the PACV characteristics of another Al_2O_3 MIS capacitor for hold time of 0–100 s under a depletion gate voltage of −16 V. The measurement for hold time of 0 s was carried out under the lighting in mode B here and in what follows. The postillumination characteristics shifted with hold time positively along the voltage axis. This shift might have been caused by the hole emission from the depopulated interface states and the valence band (inversion holes, if any) into the insulator valence band or by capturing the persistent-photoconduction electrons that were emitted from the gate, drifting in the insulator conduction band to the interface and finally flowing into the substrate.[20] The parallel *C*–*V* characteristic shifts are more clearly seen in Fig. 8, where the voltage shifts for particular t_{hold} approximately remained unchanged

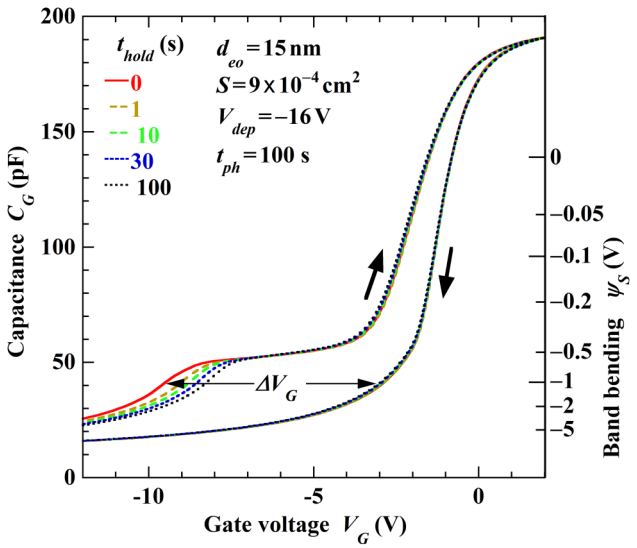

FIG. 7. PACV characteristics of an Al/Al_2O_3/GaN capacitor for various hold times. The sample was illuminated for 100 s under the depletion gate voltage of −16 V. The result for the hold time of 0 s was obtained by illuminating the sample in mode B, whereas the others were measured in mode A.

for capacitance of smaller than 40 pF. This makes a contrast to the results in Fig. 4, where the voltage shifts for illumination time of under 60 s increased with capacitance of up to 30–40 pF. The hole recombination and interface-state repopulation processes different between Figs. 3 and 7 suggest that the populations of interface states in the two figures might be different from each other. Because even the 1-s hold time appreciably reduced the voltage shifts, lighting B was adopted in what follows. Given that the voltage shift–capacitance relationship for lighting B is similar to that for the others, this type of illumination did not have any adverse effects on the C–V measurements. To remove a possible contribution from inversion holes, some previous studies secured a finite hold time.[10,12] This approach, however, is not recommended because deep interface states close to the valence band are also removed and because the shift does not easily bottom, causing a hold-time-dependent uncertainty of obtained results.

C. Choice of depletion gate voltage

The vital role played by the depletion gate voltage for accurate PACV analysis was formerly pointed out although without detailed data, requiring that the voltage should be large enough such that all interface states are located above the Fermi level, or more exactly the flat-band or bulk Fermi level.[10] This criterion is re-examined here based on the basic principle of PACV analysis. The PACV characteristics are only obtained for gate voltages that are limited by the depletion gate voltage, as specifically shown for −6 V by those in the shaded portion of Fig. 3. Figure 9 collectively shows the PACV characteristics measured for a depletion gate voltage of −4 to −16 V under the B-mode illumination for 500 s. Owing to this appropriate choice of the illumination time and the hold time, all the postillumination C–V characteristics, except that for −4 V, approximately agree with each other, irrespective of the gate voltage of under −4 V. Here, it should be noted that the minimum gate voltage of the postillumination characteristics is limited by the depletion gate voltage, as mentioned above. Therefore, all the

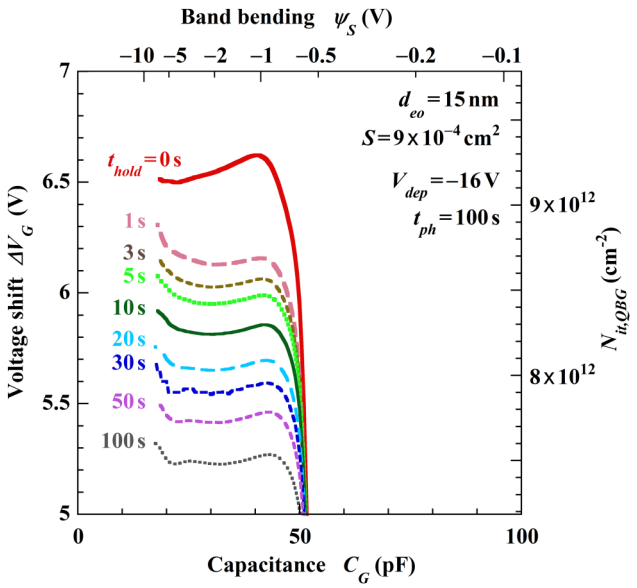

FIG. 8. Voltage shifts for various hold times. Some of the results were obtained by using the data given in Fig. 7.

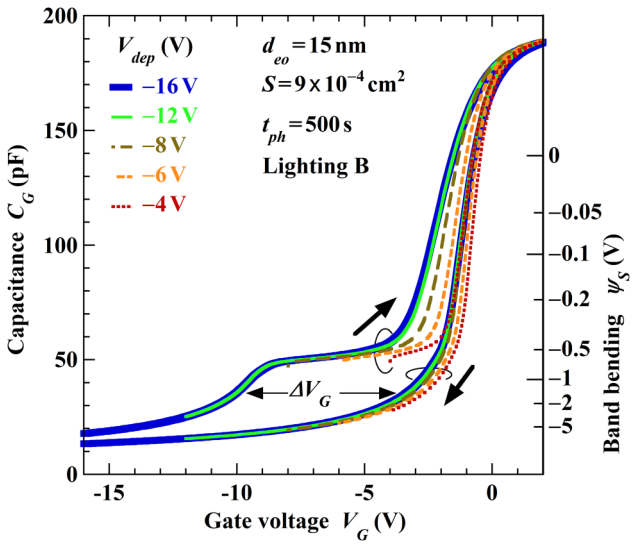

FIG. 9. PACV characteristics for various depletion gate voltages. The sample was illuminated in mode B for 500 s.

postillumination characteristics do not yield accurate results, as shown in Fig. 10, where the voltage shifts for a depletion gate voltage of −4 to −18 V are comparatively shown as a function of capacitance. Specifically, the voltage shifts for a depletion gate voltage of −8 V and larger have maximum values that are quite smaller than the others, due to the limited gate voltage range of the postillumination characteristics. For reference, the voltage shifts for shorter illumination times are approximately illustrated by the portions that have left borders represented by the thin lines (gray in color printing) in Fig. 4. Due to the Al_2O_3 charging by PACV measurements and the variation among samples, the results in Figs. 4 and 10 for the same measurement condition are slightly different from each other.

To more clearly show the effect of the depletion gate voltage, Fig. 11 shows the quasitotal interface-state densities for minimum capacitance (open triangles) and for maximum voltage shift (open squares) as a function of depletion gate voltage. It is examined in Sec. III D how to choose between these two types of quasitotal interface-state densities. Both densities approximately remain constant for a depletion gate voltage of −9 V and smaller, yielding their accurate estimation, whereas they remarkably decrease for −8 V or larger, where previous investigations were mostly carried out. As explained above (Sec. III A), these failures of accurate analysis were caused by the insufficient magnitude of band bending, as represented by the solid line in Fig. 11. Here, the values of band bending are those for the minimum capacitance in Fig. 10. Hence, we obtain a guideline for accurate PACV analysis; the depletion gate voltage for illumination should be large enough that the photoinduced voltage shift can be read at the capacitance for which the band bending in the substrate is outside the error zone,

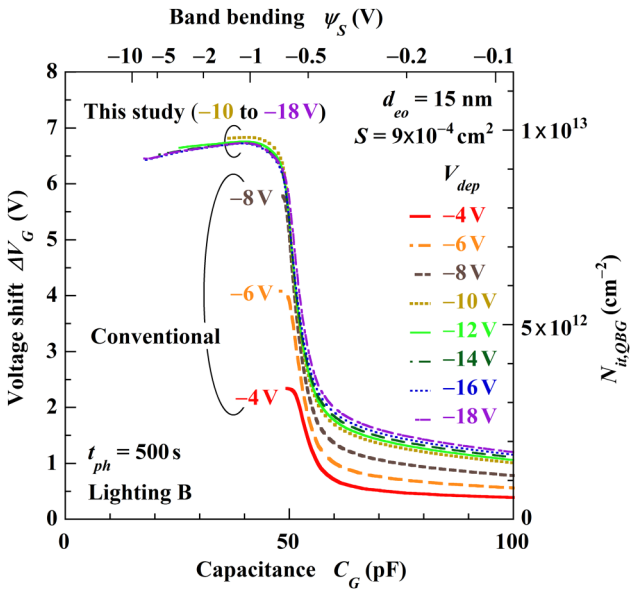

FIG. 10. Voltage shifts for various depletion gate voltages. Some of the results were obtained by using the data given in Fig. 9.

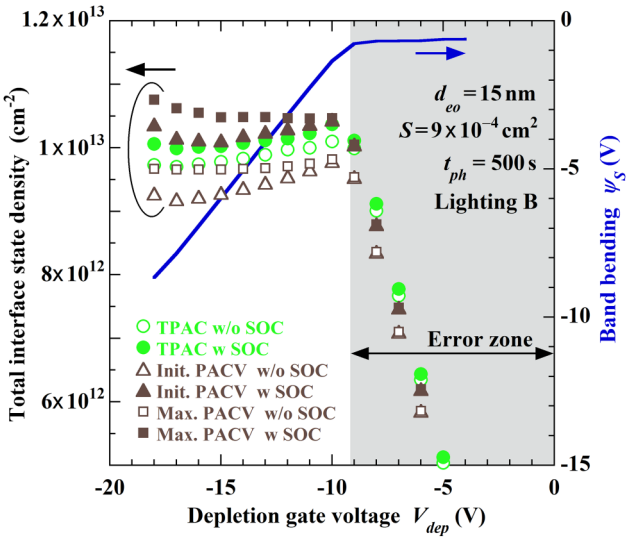

FIG. 11. Total interface-state densities before (open symbols) and after (filled ones) the correction of *C–V* stretch-out effect. The triangles, squares, and circles represent the values for the minimum capacitance, the maximum values, and TPAC results,[20] respectively. The solid line represents the band bending at the beginning of the postillumination *C–V* measurements.

i.e., $|\psi_S| > 1$ V. By contrast, the aforementioned previous guideline is equivalent to requiring that the magnitude of band bending should be larger than the bandgap divided by q, i.e., 3.4 V for GaN, being sufficient but not necessary. This excessive requirement was supposedly caused by neglecting the fact that depopulated interface states remain empty until an appreciable number of electrons are induced in the conduction band by the band bending of −0.6 V and larger.

D. Correction for *C–V* stretch-out effect

As mentioned earlier (Sec. III A), based on the photoinduced shift of *C–V* characteristics, the PACV analysis estimates the total interface-state density across the bandgap. For the results thus obtained to cover the entire bandgap, the reference *C–V* characteristics should be measured with all interface states being filled with electrons. Actually, however, some of the interface states are depopulated during the *C–V* measurements, and, therefore, the reference characteristics (open circles in Fig. 12) exhibit so-called stretch-out, being negatively shifted under depletion with respect to interface-state-free characteristics (solid line in Fig. 12). Here, although some might regard the photoinduced voltage shift as a kind of stretch-out, the usage of this term is limited in this study to the aforementioned conventional sense, i.e., the deviation of an illumination-free experimental *C–V* characteristic from an interface-state-free theoretical characteristic. For reference, instead of the latter, some authors used the former that were shifted to compare with postillumination characteristics.[10,11] This approach obviously overlooks not only the stretch-out effect but also deep interface states that are difficult to distinguish from insulator traps, and, therefore, cannot

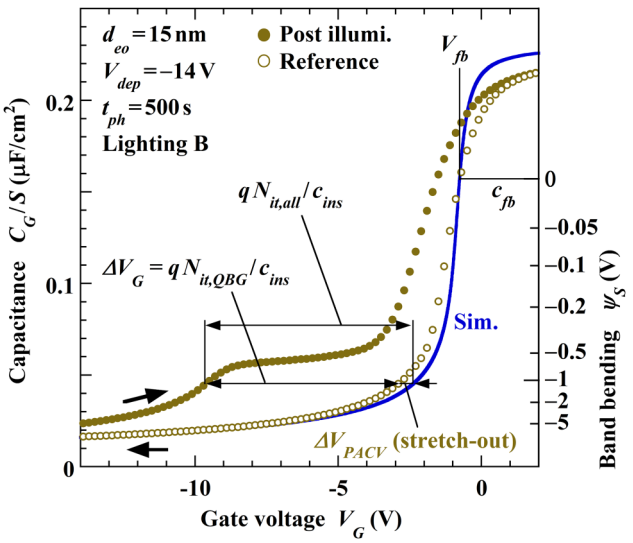

FIG. 12. PACV characteristics in comparison with an interface-state-free theoretical *C–V* characteristic. The closed and open symbols represent the postillumination and the reference characteristic, respectively, that were measured under the depletion gate voltage of −14 V. The line represents a *C–V* characteristic that was simulated by assuming no interface states but some insulator charge adjusted in such a way that the theoretical characteristic crosses the reference one at the flat-band voltage V_{fb}.

be adopted here. Returning to the stretch-out correction method, the total interface-state density obtained in Secs. III A–III C is smaller than the entire-bandgap value by the amount of ΔN_{PACV} that is determined by $\Delta N_{PACV} = c_{ins}\Delta V_{PACV}/q$ using ΔV_{PACV} (see Fig. 12). The interface-state-free *C–V* curve here is placed in such a way that the theoretical and the measured characteristic intersect at the flat-band voltage, for which the capacitance c_{fb} is equal to $1/(1/c_{ins} + \lambda_{Debye}/\varepsilon_s)$ with λ_{Debye} being the extrinsic Debye length.[22] Therefore, even after the correction for this stretch-out effect, the interface states above the Fermi level at the flat band are still excluded from the results. Despite this drawback, the aforementioned choice of theoretical *C–V* curve has an advantage of avoiding a considerable margin of error caused by inaccurate estimates of insulator EOTs. For reference, to extract the interface-state distribution in the bandgap, the Terman method utilizes the stretch-out of *C–V* characteristics. Therefore, ΔV_{PACV} is related to the interface-state density $D_{it,Terman}$, obtained by the Terman method, by

$$\Delta V_{PACV} = \frac{q}{c_{ins}} \int_{E_F + q\Psi_{S,0}}^{E_F} D_{it,Terman} dE, \tag{3}$$

where $\psi_{S,0}$ is the band bending for the capacitance at which the voltage shift is read, and E_F is the Fermi level at the flat band, being equal to $E_C - 0.10$ eV with E_C as the conduction-band edge in this study. It should be noted that $D_{it,Terman}$ increasingly underestimates the actual value deep into the bandgap. Then, the right total interface-state density $N_{it,all}$ across the bandgap is obtained by adding ΔN_{PACV} to the values obtained in Sec. III C. The closed triangles and closed squares in Fig. 11 represent the results that were obtained by applying this correction to those represented by the open triangles and open squares, respectively. For comparison, the stretch-out-corrected TPAC results are also shown in Fig. 11, as represented by the closed circles.[20] As shown in Fig. 11, for a depletion gate voltage of −9 V and smaller, the stretch-out-corrected PACV results for minimum capacitance (closed triangles) are not only approximately the same as 1.0×10^{13} cm^{-2}, which is averaged to 3.0×10^{12} cm^{-2} eV^{-1} over the GaN bandgap, but also agree quite well with the stretch-out-corrected TPAC results (closed circles), validating both the PACV and the TPAC analyses. In a sense, given that the minimum capacitance in PACV analysis was measured right after the TPAC measurement, this agreement is quite reasonable. Finally, the TPAC measurements can be simultaneously carried out with the PACV measurements without additional times as mentioned earlier (Sec. III A). The agreement between the two, as in Fig. 11, adds a great deal of credibility to obtained results.

IV. DISCUSSION

Several models of ledge formation were previously proposed,[7,9,11,23] rather *a priori* ascribing the single or major ledge to inversion carries, i.e., holes in *n*-type substrates. Here, based on the results obtained as mentioned earlier in this study, the ledge formation mechanism is re-examined. As shown in Figs. 3, 7, and 9, the interface-state or inversion-hole ledges were observed at the band bending ψ_S of approximately −0.6 to −0.5 V, for which an appreciable number of electrons available for filling depopulated interface states and for the recombination with inversion holes exist in the conduction band (Fig. 6). Based on this fact, the ledges are considered to be formed in the following way. For $\psi_S < -0.6$ V, there are only few electrons in the conduction band, and, therefore, depopulated interface states are kept empty and inversion holes, if any, are retained, thereby increasing the band bending (decreasing the magnitude) with the gate voltage in the same way as in the reference *C–V* characteristics. Due to this manner of ψ_S change, the shifted PACV curve for deep depletion is parallel to the reference. As the band bending approaches the threshold value of −0.6 V, the conduction-band electrons exponentially increase their density and begin to fill empty interface states and recombine with inversion holes. At this stage, the increased gate voltage is mostly spent on the gate insulator due to the increase in negative charge (interface states) and the decrease in positive charge (inversion holes) at the interface, with the band bending slightly increasing to −0.5 V. As a result, the capacitance approximately remains constant for these gate voltages, forming a ledge. Here, the time τ needed for an interface state or an inversion hole to capture the conduction-band electrons is given by $\tau = 1/(\sigma_{it} v_{th} n_e)$,[1] where σ_{it} is the capture cross section for electrons and v_{th} is the thermal velocity of conduction-band electrons. As the thermal velocity is of the order of 10^7 cm/s and several seconds were spent to measure the capacitance in the ledge, the cross section of the interface states or the inversion holes that captured electrons during the ledge is estimated to be of the order of 10^{-15} cm^2 for conduction-band electrons of 10^7 cm^{-3}, a typical value in the ledge. This value is much larger than the value of 10^{-19} cm^2 reported for Al_2O_3/GaN interface,[24] but consistent with

the values of 10^{-19}–10^{-14} and 10^{-17}–10^{-13} cm^2 for SiO_2/SiC[25–27] and SiO_2/Si interface,[28–30] respectively. Since the number of articles on the capture cross section of Al_2O_3/GaN interface states is very limited and the aforementioned cross sections for SiO_2/SiC and SiO_2/Si were distributed by 4–5 orders of magnitude, we cannot rule out the possibility that future studies will report the values comparable to ours. After the electrons fill the deep interface states and recombine with the inversion holes, the increased gate voltage is again imposed mostly on the substrate. This increases the band bending and the capacitance as well. Now the interface states are approximately in thermal equilibrium, and the larger the band bending (smaller magnitude) is, the closer to the thermal equilibrium the system is. In this way, above the ledge, the distribution of interface states can be scanned in the bandgap by using PACV results, in the same way as by the Terman method. However, due to the limited time available for capturing conduction-band electrons, the number of re-populated interface states is smaller than that expected in thermal equilibrium. This means that the interface-state densities obtained by using PACV results[10,11] overestimate actual values, in a manner similar to the way the Terman method underestimates them.

As obviously seen from the aforementioned ledge formation mechanism, the ledge extent is approximately proportional to the number of inversion holes and deep interface states, which are located below about 0.5 eV from the flat-band Fermi level. The magnitude of band bending for the ledge formation is supposed to increase with electron capture cross section of deep interface states and inversion holes, since a larger cross section only necessitates fewer electrons, i.e., a larger magnitude of band bending, for the recombination with and the capture of the conduction-band electrons in a limited time during the C–V measurements. These understandings help us investigate the origin of the ledges observed in this study in the following way. When both deep interface states and inversion holes exist and have different cross sections, two ledges are expected to be formed, as previously observed using p-type[7,9,23] and n-type[23] SiC capacitors. Since the band offsets for inversion carriers in these studies were larger than those of Al_2O_3/GaN, the coexistence of deep interface states and inversion holes is likely, although it still needs to be further investigated, as done in this study. By contrast, this and some previous studies[11] observed only a single ledge for Al_2O_3/GaN capacitors. This result points to two possibilities. The one is that both deep interface states and inversion holes exist and have the same cross section. Seeing that SiC PACV results had two ledges, this model seems less likely. The other possibility is that either deep interface states or inversion holes exclusively exist, regardless of their cross sections. To judge which one is the case, attention should be paid to a recent report, although not for Al_2O_3/GaN, that the interface-state density at SiO_2/GaN is of the order of 10^{13} cm^{-2} eV^{-1} for $E_C - E$ of 2–3.4 eV,[31] where E is the energy level of the interface states. This density is large enough to cause the ledge as observed in this and previous studies. Additionally, besides the field emission, the inversion holes are also depopulated by the photo-excitation, as schematically shown in Figs. 2(b) and 2(c), suggesting negligible hole inversion. Here, it should be noted that the photons for this process only need an energy of the valence band offset, i.e., approximately 1.8 eV (actually less than this), and are much more abundant than those for electron–hole pair generation in this study. Therefore, the deep interface states are the most probable candidate for the ledge formation in this study.

In the framework of the aforementioned ledge formation mechanism, the interface states detected above the ledges, as in most previous studies, were only those that were located not much deeper than the aforementioned energy level for the ledges, i.e., 0.6 eV below the flat-band Fermi level. This detection range of interface states was approximately the same as that of the Terman method. Additionally, due to the C–V stretch-out effect, the conventional PACV method even underestimated the aforementioned relatively shallow interface states, being ruled out as the method for detecting deep interface states. For reference, most previous studies on GaN capacitors[32–35] reported PACV characteristics quite similar to those for over-80-s illumination in the voltage range of −6 to 2 V, as shown in Fig. 3 (shaded portions). These results apparently indicated that the pinned band bending in the substrate would have been kept even for a larger magnitude of depletion gate voltage. This limited pinning led to the conclusion that the photoinduced capacitance enhancement was caused by inversion holes and to the claim that the samples in those studies had a small number of interface states, based on the small voltage shift observed for the capacitance above the ledge, e.g., 60 pF in Fig. 3. Actually, however, for a larger magnitude of depletion gate voltage, the band bending was no more pinned, as shown by the unshaded results in Fig. 3 and by previous results.[11] The guidelines proposed in this study help re-examine these studies.

V. CONCLUSIONS

To accurately analyze the deep states at the insulator/wide-bandgap semiconductor interface, we reassessed and improved the conventional photoassisted C–V (PACV) method, as summarized in what follows. First, as previously pointed out, the illumination time under depletion should be long enough that the voltage shift caused by interface-state depopulation saturates (in n-type semiconductors). Excessive illumination, however, causes insulator charging, thereby apparently increasing estimated values. To solve this problem, this study proposes to measure reference C–V characteristics after postillumination ones. Secondly, contrary to previous approaches, the postillumination (depletion-to-accumulation) C–V measurements should be started without delay after turning off the light or may be carried out with the samples being illuminated, to suppress the repopulation of depopulated interface states (in n-type). Thirdly, the depletion should be deep enough that the band bending in the substrate at the beginning of the postillumination C–V measurements is outside the error zone (over −1 V in n-type). This guideline considerably relaxes a previous one that required a band bending larger than the bandgap. Furthermore, this study developed a method for compensating for the interface-state depopulation (in n-type) during the reference C–V measurements, in which the depopulation causes the so-called stretch-out. The results thus obtained from an Al/Al_2O_3/GaN capacitor agreed fairly well with those by a recently developed transient photoassisted capacitance method, yielding the average interface-state density of 3.0×10^{12} cm^{-2} eV^{-1}. Based on these results, a ledge formation model is presented, suggesting the practical absence of inversion holes (in n-type) and estimating the electron capture cross section of

interface states at Al_2O_3/GaN in this study to be of the order of 10^{-15} cm^2. Being less sensitive to the gate-insulator charging, the advanced PACV method developed in this study has an advantage over the transient method and, therefore, will help enhance the technology for fabricating high-performance, high-reliability insulator/wide-bandgap semiconductor interfaces.

ACKNOWLEDGMENTS

This research is supported by the "Program for Research and Development of Next-Generation Semiconductor to Realize Energy-Saving Society" and the "Project of Creation of Life Innovation Materials for Interdisciplinary and International Researcher Development" of the Ministry of Education, Culture, Sports, Science and Technology (MEXT), Japan. The sample preparation and measurements were performed at the Research Organization for Nano and Life Innovation (RONLI) of Waseda University.

REFERENCES

[1]S. M. Sze and K. K. Ng, *Physics of Semiconductor Devices*, 3rd ed. (Wiley, Hoboken, NJ, 2007).
[2]E. H. Nicollian and J. R. Brews, *MOS (Metal Oxide Semiconductor) Physics and Technology* (Wiley, New York, 1982).
[3]C. N. Berglund, IEEE Trans. Electron Devices **13**, 701 (1966).
[4]L. M. Terman, Solid-State Electron. **5**, 285 (1962).
[5]R. Castagné and A. Vapaille, Surf. Sci. **28**, 157 (1971).
[6]E. H. Nicollian and A. Goetzberger, Bell Syst. Tech. J. **46**, 1055 (1967).
[7]J. A. Cooper, Jr., Phys. Status Solidi A **162**, 305 (1997).
[8]H. C. Casey, Jr., G. G. Fountain, R. G. Alley, B. P. Keller, and S. P. DenBaars, Appl. Phys. Lett. **68**, 1850 (1996).
[9]J. Tan, M. K. Das, J. A. Cooper, and M. R. Melloch, Appl. Phys. Lett. **70**, 2280 (1997).
[10]B. L. Swenson and U. K. Mishra, J. Appl. Phys. **106**, 064902 (2009).
[11]R. Yeluri, X. Liu, B. L. Swenson, J. Lu, S. Keller, and U. K. Mishra, J. Appl. Phys. **114**, 083718 (2013).
[12]A. Winzer, N. Szabó, A. Wachowiak, P. M. Jordan, J. Heitmann, and T. Mikolajick, J. Vac. Sci. Technol. B **33**, 01A106 (2015).
[13]A. Hiraiwa, T. Sasaki, S. Okubo, K. Horikawa, and H. Kawarada, J. Appl. Phys. **123**, 155303 (2018).
[14]A. Hiraiwa, T. Saito, D. Matsumura, and H. Kawarada, J. Appl. Phys. **117**, 215304 (2015).
[15]T. Ando, A. B. Fowler, and F. Stern, Rev. Mod. Phys. **54**, 437 (1982).
[16]A. Hiraiwa, S. Sakai, D. Ishikawa, and M. Nakazawa, J. Appl. Phys. **91**, 6571 (2002).
[17]A. Hiraiwa, A. Shima, and D. Ishikawa, IEEE Trans. Electron Devices **58**, 650 (2011).
[18]A. Hiraiwa, D. Matsumura, and H. Kawarada, J. Appl. Phys. **120**, 084504 (2016).
[19]B. S. Eller, J. Yang, and R. J. Nemanich, J. Vac. Sci. Tehcnol. A **31**, 050807 (2013).
[20]A. Hiraiwa, S. Okubo, K. Horikawa, and H. Kawarada, "Transient photo-assisted capacitance characterization of insulator/wide-bandgap semiconductor interface using super-bandgap illumination," J. Appl. Phys. (submitted).
[21]S. O'Leary, B. Foutz, M. Shur, and L. Eastman, J. Mater. Sci. Mater. Electron. **17**, 87 (2006).
[22]D. K. Schroder, *Semiconductor Material and Device Characterization* (Wiley, NJ, 2006).
[23]H. Yano, F. Katafuchi, T. Kimoto, and H. Matsunami, IEEE Trans. Electron Devices **46**, 504 (1999).
[24]K. Ooyama, H. Kato, M. Miczek, and T. Hashizume, Jpn. J. Appl. Phys. **47**, 5426 (2008).
[25]P. A. Ivanov, T. P. Samsonova, V. N. Panteleev, and D. Y. Polyakov, Semiconductors **35**, 468 (2001).
[26]X. D. Chen, S. Dhar, T. Isaacs-Smith, J. R. Williams, L. C. Feldman, and P. M. Mooney, J. Appl. Phys. **103**, 033701 (2008).
[27]H. Yoshioka, T. Nakamura, and T. Kimoto, J. Appl. Phys. **112**, 024520 (2012).
[28]W. Fahrner and A. Goetzberger, Appl. Phys. Lett. **17**, 16 (1970).
[29]H. Deuling, E. Klausmann, and A. Goetzberger, Solid-State Electron. **15**, 559 (1972).
[30]J. A. Cooper and R. J. Schwartz, Solid-State Electron. **17**, 641 (1974).
[31]A. Ohta, N. X. Truyen, N. Fujimura, M. Ikeda, K. Makihara, and S. Miyazaki, Jpn. J. Appl. Phys. **57**, 06KA08 (2018).
[32]T. Hashizume, E. Alekseev, D. Pavlidis, K. S. Boutros, and J. Redwing, J. Appl. Phys. **88**, 1983 (2000).
[33]B. Gaffey, L. J. Guido, X. W. Wang, and T. P. Ma, IEEE Trans. Electron Devices **48**, 458 (2001).
[34]C. Bae and G. Lucovsky, J. Vac. Sci. Technol. A **22**, 2402 (2004).
[35]Y. Q. Wu, T. Shen, P. D. Ye, and G. D. Wilk, Appl. Phys. Lett. **90**, 143504 (2007).